

## On meson spectral functions at high temperature and nonzero momentum

---

**Gert Aarts<sup>‡</sup>, Simon Hands<sup>§</sup>**

*University of Wales Swansea*

*E-mail: g.aarts@swan.ac.uk, s.hands@swan.ac.uk*

**Seyong Kim**

*Sejong University, Seoul*

*E-mail: skim@sejong.ac.kr*

**Jose M. Martínez Resco**

*Brandon University*

*E-mail: martinezrescoj@brandonu.ca*

In the high-temperature phase of QCD meson spectral functions at nonzero momentum are expected to have a nontrivial and interesting structure. In order to provide a reference point for lattice studies employing e.g. the Maximal Entropy Method, we discuss several characteristics of meson spectral functions in the infinite-temperature limit. We report on ongoing work in quenched QCD with staggered fermions.

*XXIIIrd International Symposium on Lattice Field Theory*

*25-30 July 2005*

*Trinity College, Dublin, Ireland*

---

\*Speaker.

<sup>‡</sup>PPARC Advanced Fellow

<sup>§</sup>PPARC Senior Research Fellow

## 1. Spectral functions

The recent experimental progress in the recreation of the quark gluon plasma in relativistic heavy ion collisions (see e.g. [1]) has been an important stimulus for lattice studies of spectral functions in the high-temperature phase of QCD. Topics discussed so far (ordered according to increasing difficulty) include the persistent presence of charmonium bound states above the deconfinement transition [2, 3, 4], the thermal dilepton rate [5], and transport coefficients, such as the electrical conductivity [6] and the shear viscosity [7]. In spectral function calculations soft energies  $\omega \lesssim T$  are of particular interest, since this is where one expects e.g. nonperturbative medium effects and collective excitations, predicted by perturbative studies of hot QCD. Moreover, transport coefficients follow from current-current spectral functions in the limit of vanishing energy (Kubo relations). So far numerical results for the soft energy region in the high-temperature phase are rather scarce. For the dilepton rate, it was found [5] (surprisingly) that the spectral function in the vector channel  $\rho_V(\omega, \mathbf{0})$  is consistent with zero when  $\omega \lesssim 2T$ . For the electrical conductivity,  $\rho^{ii}(\omega, \mathbf{0})$  was reconstructed at low energies [6] and a structure resembling analytical expectations [8] was obtained.

However, numerically determined euclidean correlators  $G_H(\tau, \mathbf{p})$  do not easily provide knowledge of spectral functions at soft energies. In fact, they are largely insensitive to details of  $\rho_H(\omega, \mathbf{p})$  in this region because the kernel  $K$ , which relates  $G_H$  and  $\rho_H$  via

$$G_H(\tau, \mathbf{p}) = \int_0^\infty \frac{d\omega}{2\pi} K(\tau, \omega) \rho_H(\omega, \mathbf{p}), \quad K(\tau, \omega) = \frac{\cosh[\omega(\tau - 1/2T)]}{\sinh(\omega/2T)}, \quad (1.1)$$

becomes independent of  $\tau$  for smaller energies ( $K(\tau, \omega) \sim 2T/\omega$  when  $\omega \ll T$ ). It follows in particular that lattice correlators are remarkably insensitive to transport coefficients [8] (see ref. [9] for a recent analysis reaching the same conclusion). In view of the experimental results on the strongly interacting QGP, suggesting e.g. a surprisingly small shear viscosity, it is important to gain more experience in the reconstruction of spectral functions at energies  $\omega \lesssim T$  from lattice QCD.

Good candidates for such studies are meson spectral functions at nonzero momentum  $p$  [10]. Because of the presence of the lightcone at  $\omega = p$  and the nontrivial spectral weight below the lightcone, commonly referred to as Landau damping and due to the scattering of quarks with off-shell gauge bosons, they are expected to have an interesting structure at soft energies. By choosing the nonzero momentum  $p$  of the order of  $T$  or larger, the region below the lightcone can be made sufficiently large and (part of) the difficulties present for transport coefficients, inherent in the strict limit  $\omega \rightarrow 0$ , can be circumvented. In order to provide a reference point for such calculations, we studied meson spectral functions at nonzero momentum in the infinite temperature limit, both in the continuum and on the lattice for Wilson and staggered (naive) fermions [10]. A similar study at zero momentum can be found in ref. [11]. Below we summarize some of our findings. In the outlook we report on ongoing work in quenched QCD with staggered fermions.

## 2. Infinite temperature

We consider meson spectral functions  $\rho_H(t, \mathbf{x}) = \langle [J_H(t, \mathbf{x}), J_H^\dagger(0, \mathbf{0})] \rangle$  at leading order in the loop expansion. The currents in the various channels are given by  $J_H(t, \mathbf{x}) = \bar{q}(t, \mathbf{x}) \Gamma_H q(t, \mathbf{x})$  with

$\Gamma_H = \{\mathbb{1}, \gamma_5, \gamma^\mu, \gamma^\mu \gamma_5\}$ . In the continuum the one-loop integral

$$\rho_H(\omega, \mathbf{p}) = -2\text{Im} T \sum_{l \in \mathbb{Z}} \int \frac{d^3k}{(2\pi)^3} \text{tr} S(i\tilde{\omega}_l, \mathbf{k}) \Gamma_H S(i\omega_n + i\tilde{\omega}_l, \mathbf{p} + \mathbf{k}) \gamma^0 \Gamma_H^\dagger \gamma^0 \Big|_{i\omega_n \rightarrow \omega + i0^+}, \quad (2.1)$$

where  $S(i\tilde{\omega}_l, \mathbf{k})$  is the fermion propagator, can be done analytically, for arbitrary external momentum  $p$  and fermion mass  $m$ . Since the outcome is rather lengthy, we refer to ref. [10] for detailed expressions. On the lattice completely analytical results are not available, but simple expressions which are easily evaluated numerically can be given. In order to do so, we use a 'mixed' representation [12] and write the fermion propagator as  $S(\tau, \mathbf{k}) = \gamma_4 S_4(\tau, \mathbf{k}) + \sum_{i=1}^3 \gamma_i S_i(\tau, \mathbf{k}) + \mathbb{1} S_u(\tau, \mathbf{k})$ . For Wilson fermions, the  $S(\tau, \mathbf{k})$  functions depend on  $\tau$  via  $\sinh(\tilde{\tau} E_{\mathbf{k}})$  and  $\cosh(\tilde{\tau} E_{\mathbf{k}})$ , where  $\tilde{\tau} = \tau - 1/2T$ , which makes it straightforward to arrive at the relationship (1.1), also on a finite lattice. The resulting spectral functions are then given by a sum over the spatial lattice momenta, which can be done numerically.

For naive fermions there are a few changes, due to the time doublers. The hyperbolic functions are now multiplied with the staggering factors  $1 \pm (-1)^{\tau/a_\tau}$ , such that relation (1.1) is modified to

$$G_H(\tau, \mathbf{p}) = 2 \int_0^\infty \frac{d\omega}{2\pi} K(\tau, \omega) \left[ \rho_H(\omega, \mathbf{p}) - (-1)^{\tau/a_\tau} \tilde{\rho}_H(\omega, \mathbf{p}) \right], \quad (2.2)$$

where  $K$  is again the same kernel as in the continuum. The staggered partner  $\tilde{\rho}_H$  is related to  $\rho_H$  via the replacement  $\Gamma_H \rightarrow \tilde{\Gamma}_H = \gamma_4 \gamma_5 \Gamma_H$ .

We now discuss several characteristics. It is expected from naive dimensional arguments that meson spectral functions increase with  $\omega^2$  for large  $\omega$ . This is demonstrated in fig. 1 (top), where we show the (pseudo)scalar spectral functions  $\rho_{\text{PS},\text{S}}(\omega, \mathbf{p})$ , normalized with  $\omega^2$ , in the continuum and on the lattice for finite  $N_\tau = 16$ . In order to approximate the thermodynamic limit,  $N_\sigma$  is taken very large, typically  $\sim 2000$  [10]. We only show results for isotropic lattices here, results for anisotropic lattices can be found in ref. [10]. The cusps at larger energies are due to the finite Brillouin zone and are therefore lattice artefacts. They are located at  $\omega = E_{\mathbf{k}-\mathbf{p}/2} + E_{\mathbf{k}+\mathbf{p}/2} \approx 2E_{\mathbf{k}}$ ,

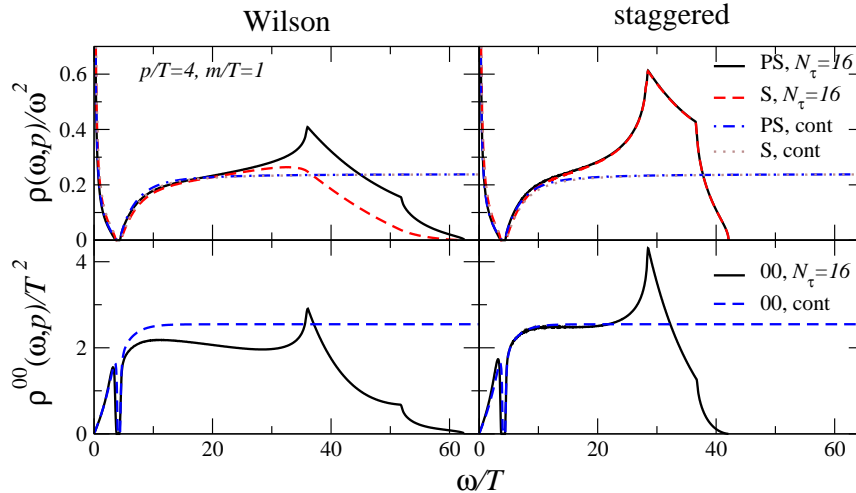


**Figure 1:** Pseudoscalar and scalar spectral functions  $\rho_{\text{PS},\text{S}}(\omega, \mathbf{p})/\omega^2$  (top) and charge density spectral functions  $\rho^{00}(\omega, \mathbf{p})/T^2$  (bottom) as a function of  $\omega/T$ .

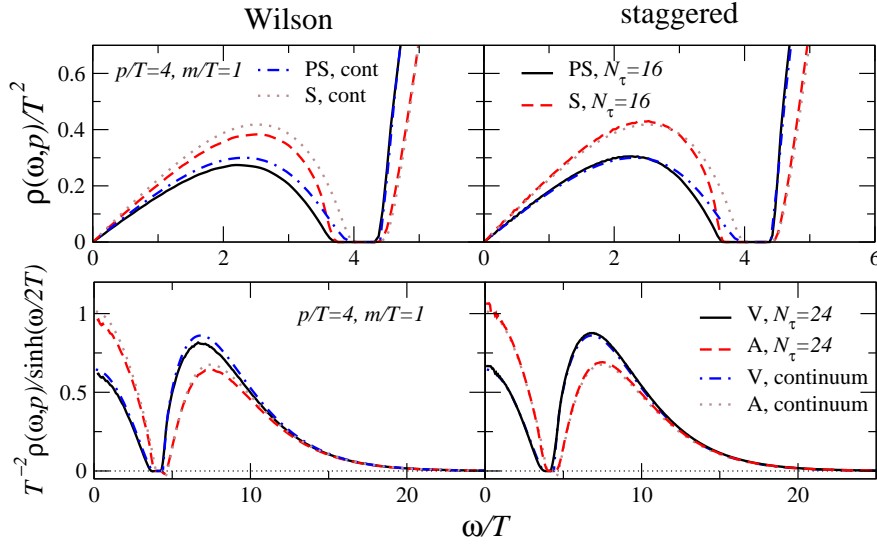


**Figure 2:** Low energy region of  $\rho_{\text{PS,S}}(\omega, \mathbf{p})$ , normalized with  $T^2$ , from fig. 1 (top) and  $\rho_{\text{V,A}}(\omega, \mathbf{p})$ , normalized with  $T^2 \sinh(\omega/2T)$ , (bottom) as a function of  $\omega/T$ .

with  $\mathbf{k} = (\pi/a, 0, 0), (\pi/a, \pi/a, 0) + \text{permutations}$  for Wilson fermions. The maximal energy is determined by  $\mathbf{k} = (\pi/a, \pi/a, \pi/a)$  ( $\mathbf{k} = (\pi/2a, \pi/2a, \pi/2a)$  for staggered fermions). For Wilson fermions  $\rho_{\text{PS}}$  and  $\rho_{\text{S}}$  differ, due to the presence of the Wilson mass term, while for staggered and continuum fermions they are degenerate for larger energies.

Charge density spectral functions do not increase with  $\omega^2$ , but instead reach a constant value:  $\rho^{00}(\omega, \mathbf{p}) \rightarrow N_c p^2 / 6\pi$  (vector charge density) and  $\rho_5^{00}(\omega, \mathbf{p}) \rightarrow N_c (p^2 + 6m^2) / 6\pi$  (axial charge density). Note that this is relevant for the choice of default model in the Maximal Entropy Method [13]. For the vector charge density, this large energy behaviour follows from current conservation. In fact, at zero momentum current conservation completely fixes the charge density spectral function to be  $\rho^{00}(\omega, \mathbf{0}) = 2\pi\chi\omega\delta(\omega)$ , where  $\chi$  is the charge susceptibility. The corresponding euclidean correlator is then constant,  $G^{00}(\tau, \mathbf{0}) = T\chi$ . On the lattice these expressions only hold when the conserved current is used, and not the local one. The continuum and lattice spectral functions  $\rho^{00}$  are compared in fig. 1 (bottom) for nonzero  $p = 4T$ . Note that the local definition is used here. The staggered result appears to track the continuum one up to larger energies than the one obtained with Wilson fermions.

Clearly visible in fig. 1 is the lightcone is at  $\omega = p = 4T$  and the spectral weight below the lightcone. In the (pseudo)scalar channel, a better way to view this physically interesting region is by normalizing  $\rho_{\text{PS,S}}(\omega, \mathbf{p})$  with  $T^2$  instead of with  $\omega^2$ . The result is shown in fig. 2 (top). The spectral functions increase linearly with  $\omega$  for small  $\omega$  and vanish at the lightcone. There is a gap when  $p < \omega < \sqrt{p^2 + 4m^2}$  (higher loop corrections will fill this gap). The scalar and pseudoscalar spectral functions differ due to the nonzero quark mass. Again the staggered result compares better with the continuum one. The main lattice artefact in this region is the mismatch between the continuum and the lattice lightcone, which can be quite substantial.

A very convenient way to present both the low and the high energy behaviour of spectral functions in one figure is to show  $\rho_H(\omega, \mathbf{p}) / \sinh(\omega/2T)$ , i.e. the integrand in eq. (1.1) at the

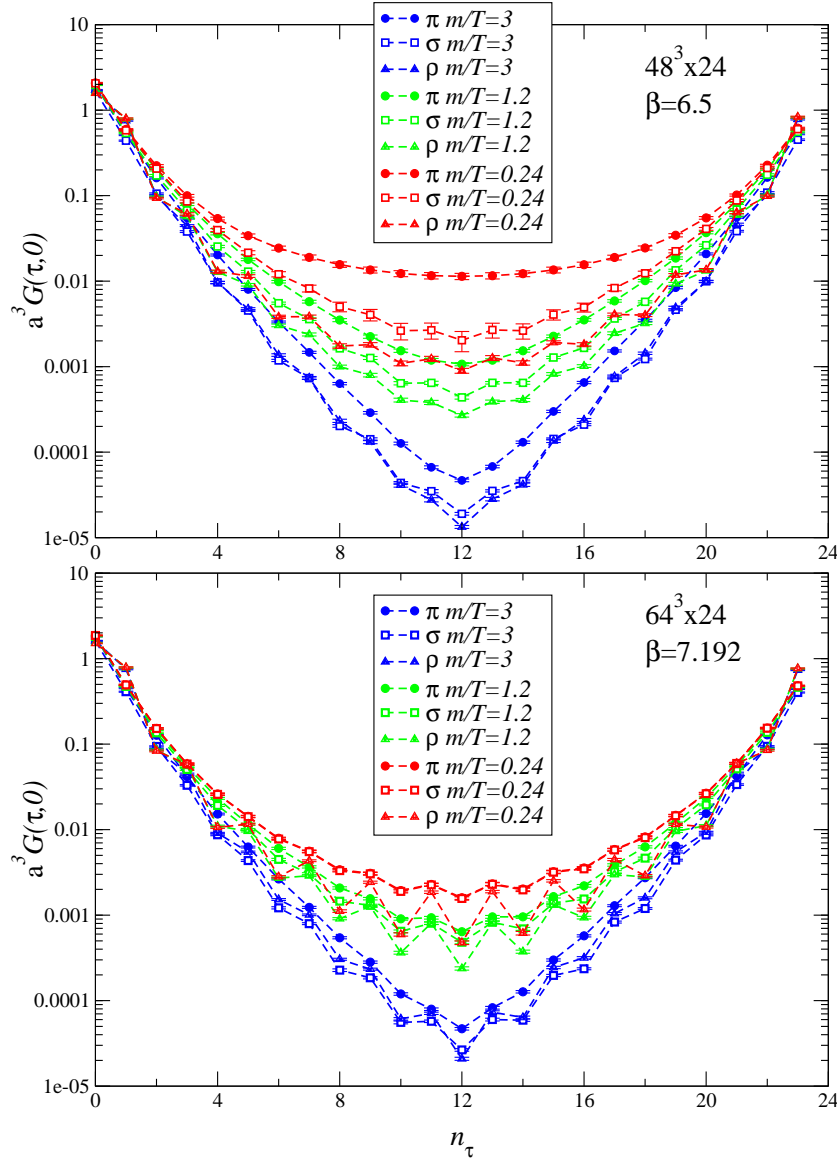


**Figure 3:** Euclidean correlators in the pseudoscalar ( $\pi$ ), scalar ( $\sigma$ ) and local vector ( $\rho$ , averaged over  $i = 1, 2, 3$ ) channel for three values of the staggered fermion mass  $m$  (in units of the temperature) in quenched QCD on a lattice with  $T \approx 160$  MeV (top) and  $T \approx 420$  MeV (bottom).

midpoint  $\tau = 1/2T$ . This combination takes a finite value when  $\omega \rightarrow 0$  and vanishes exponentially for large  $\omega$ . We show  $\rho_V = \rho^{ii} - \rho^{00}$  and  $\rho_A = \rho_5^{ii} - \rho_5^{00}$  in fig. 2 (bottom). The lattice artefacts at large  $\omega$  are now exponentially suppressed, which implies that the euclidean correlator around  $\tau = 1/2T$  is not very sensitive to those. Finally, the area under the two curves is identical, which follows from a surprising relation (“sum rule”) at this order in the loop expansion [10].

### 3. Outlook

In Fig. 3 we show preliminary results from a quenched simulation with staggered lattice

fermions. To facilitate comparison of hadron correlators at differing temperatures, the lattice parameters have been chosen to reproduce temperatures both below ( $\beta = 6.5$ ,  $48^3 \times 24$ ) and above ( $\beta = 7.192$ ,  $64^3 \times 24$ ) the deconfining temperature with the same number of temporal spacings  $N_\tau = 24$ . The data shown are for zero spatial momentum; comparison of the  $\pi$  and  $\sigma$ -propagators between the two sets, particularly for the lightest mass  $m/T = 0.24$  (shown in red), show clear evidence for chiral symmetry restoration in the deconfined phase. A spectral function analysis of these data using the Maximal Entropy Method is in progress.

## Acknowledgements

S.K. thanks PPARC for support during his visit to Swansea in 2004/05.

## References

- [1] K. Adcox *et al.* [PHENIX Collaboration], *Formation of dense partonic matter in relativistic nucleus nucleus collisions at RHIC: Experimental evaluation by the PHENIX collaboration*, *Nucl. Phys. A* **757** (2005) 184 [nucl-ex/0410003]; J. Adams *et al.* [STAR Collaboration], *Experimental and theoretical challenges in the search for the quark gluon plasma: The STAR collaboration's critical assessment of the evidence from RHIC collisions*, *ibid* **757** (2005) 102 [nucl-ex/0501009].
- [2] M. Asakawa and T. Hatsuda,  *$J/\psi$  and  $\eta_c$  in the deconfined plasma from lattice QCD*, *Phys. Rev. Lett.* **92** (2004) 012001 [hep-lat/0308034].
- [3] S. Datta, F. Karsch, P. Petreczky and I. Wetzorke, *Behavior of charmonium systems after deconfinement*, *Phys. Rev. D* **69** (2004) 094507 [hep-lat/0312037].
- [4] T. Umeda, K. Nomura and H. Matsufuru, *Charmonium at finite temperature in quenched lattice QCD*, *Eur. Phys. J. C* **39S1** (2005) 9 [hep-lat/0211003].
- [5] F. Karsch, E. Laermann, P. Petreczky, S. Stickan and I. Wetzorke, *A lattice calculation of thermal dilepton rates*, *Phys. Lett. B* **530** (2002) 147 [hep-lat/0110208].
- [6] S. Gupta, *The electrical conductivity and soft photon emissivity of the QCD plasma*, *Phys. Lett. B* **597** (2004) 57 [hep-lat/0301006].
- [7] A. Nakamura and S. Sakai, *Transport coefficients of gluon plasma*, *Phys. Rev. Lett.* **94** (2005) 072305 [hep-lat/0406009].
- [8] G. Aarts and J. M. Martínez Resco, *Transport coefficients, spectral functions and the lattice*, *JHEP* **0204** (2002) 053 [hep-ph/0203177]; *Transport coefficients from the lattice?*, *Nucl. Phys. Proc. Suppl.* **119** (2003) 505 [hep-lat/0209033].
- [9] P. Petreczky and D. Teaney, *Heavy quark diffusion from the lattice*, hep-ph/0507318.
- [10] G. Aarts and J. M. Martínez Resco, *Continuum and lattice meson spectral functions at nonzero momentum and high temperature*, *Nucl. Phys. B* **726** (2005) 93 [hep-lat/0507004].
- [11] F. Karsch, E. Laermann, P. Petreczky and S. Stickan, *Infinite temperature limit of meson spectral functions calculated on the lattice*, *Phys. Rev. D* **68** (2003) 014504 [hep-lat/0303017].
- [12] D. B. Carpenter and C. F. Baillie, *Free Fermion Propagators And Lattice Finite Size Effects*, *Nucl. Phys. B* **260** (1985) 103.
- [13] M. Asakawa, T. Hatsuda and Y. Nakahara, *Maximum entropy analysis of the spectral functions in lattice QCD*, *Prog. Part. Nucl. Phys.* **46** (2001) 459 [hep-lat/0011040].